Pump wavelength-dependent terahertz spin-to-charge conversion in CoFeB/MgO Rashba interface

Artem Levchuk, Vincent Juvé, Tadele Orbula Otomalo, Théophile Chirac, Olivier Rousseau, Aurélie Solignac, Gwenaëlle Vaudel, Pascal Ruello, Jean-Yves Chauleau, Michel Viret

Applied Physics Letters

RESEARCH ARTICLE | JULY 07 2023

Pump wavelength-dependent terahertz spin-to-charge conversion in CoFeB/MgO Rashba interface

Artem Levchuk ; Vincent Juvé ; Tadele Orbula Otomalo ; Théophile Chirac ; Olivier Rousseau ; Aurélie Solignac; Gwenaëlle Vaudel ; Pascal Ruello ; Jean-Yves Chauleau ; Michel Viret

Appl. Phys. Lett. 123, 012407 (2023)
https://doi.org/10.1063/5.0144645

Applied Physics Letters ARTICLE pubs.aip.org/aip/apl

Pump wavelength-dependent terahertz spin-to-charge conversion in CoFeB/MgO Rashba interface

Cite as: Appl. Phys. Lett. **123**, 012407 (2023); doi: 10.1063/5.0144645
Submitted: 31 January 2023 · Accepted: 17 June 2023 ·
Published Online: 7 July 2023

Artem Levchuk,[1,2] Vincent Juvé,[1,a)] Tadele Orbula Otomalo,[1] Théophile Chirac,[2] Olivier Rousseau,[2] Aurélie Solignac,[2] Gwenaëlle Vaudel,[1] Pascal Ruello,[1] Jean-Yves Chauleau,[2,a)] and Michel Viret[2]

AFFILIATIONS

[1]Institut des Molécules et Matériaux du Mans, UMR 6283 CNRS, Le Mans Université, 72085 Le Mans, France
[2]SPEC, CEA, CNRS, Université Paris-Saclay, 91191 Gif-sur-Yvette, France

[a)]**Authors to whom correspondence should be addressed:** vincent.juve@univ-lemans.fr and jean-yves.chauleau@cea.fr

ABSTRACT

Spin/charge interconversion mechanisms provide an essential handle to generate and detect spin currents. Their applications at different timescales are critical in spintronics since they cover a technologically relevant broadband spectrum. While the inverse spin Hall effect is known to be robust from quasi-static to sub-picosecond timescales, the conversion efficiency evolution of the inverse Edelstein effect has not been addressed yet. In this work, we report that while the quasi-static response of the inverse Edelstein effect can be comparable to that of the most efficient inverse spin Hall systems, a drastic drop of efficiency is observed in the terahertz (THz) regime. This behavior at the sub-picosecond timescale is qualitatively understood from the dependence of the inverse Edelstein effect on the energy distribution of spin-carrier entities, which is different between thermalized carriers in the quasi-static regime and hot carriers generated by light pulses. This finding is supported by the pump-laser wavelength dependence in the THz regime for the inverse Edelstein effect, which offers a promising route for tunability of spintronic devices.

Writing, storage, processing, and reading of information encoded in electronic spins are the fundamentals of a broad and active field of research: *spintronics*.[1] Its essence mainly relies on the concept of transport and flow of spin angular momentum. Such "*spin current*" is conventionally carried by conduction electrons experiencing spin-dependent scattering, leading to important effects, such as magneto-resistance and spin-transfer torque. The latest developments in the field aim to decorrelate the spin flow from the electronic charge current, leading to the concept of "pure" spin current, where the spin information is transported without its charge counterpart. The local manipulation of spin information at the nanoscale promises a tremendous reduction in Joule heating as no electrical charge is transported. Moreover, spin currents can be handled on extended time scales ranging from quasi-static manipulation down to a few tens of femtoseconds. Indeed, transport of spin angular momentum by light-induced hot electrons has been put forward as a key mechanism[2–4] in ultrafast magnetization dynamics.[5–7] This is of great potential for information processing in the picosecond regime with minimum energy consumption. Therefore, the terahertz (THz) frequency range (from 0.1 to 10 THz) is strategically important to tackle the upcoming challenges of tomorrow's information and communication technologies.[8]

Whenever pure spin currents are involved, their efficient conversion into measurable electric currents or voltages is essential. There are several spin/charge (S/C) interconversion mechanisms, all based on the spin–orbit interaction. Nowadays, the most emblematic one is the inverse spin Hall effect[9,10] (ISHE), present in conductors with large spin–orbit coupling, such as Pt or W. It is weak in 3d ferromagnets that possess a much smaller spin–orbit interaction than, e.g., 5d metals, whereas another spin–orbit scattering effect, called the anomalous Hall effect[11] (AHE), generally takes place. More recently, a distinct mechanism based on the Rashba effect, known as spin galvanic or inverse Edelstein effect (IEE),[12–15] has been used for spin-to-charge conversion. It relies on the locking between momentum and spin of conduction electrons in a two-dimensional state subjected to a strong built-in electric field. The Rashba Hamiltonian splits an ideal parabolic band into two sub-bands with opposite chiral spin structures. Pumping a dynamical spin population in such a system generates a transverse electrical current, thus acting as a S/C convertor.[16]

One of the latest breakthroughs in spintronics and THz technologies is the combined use of ultrafast hot electron transport and S/C conversion mechanisms. During light-induced demagnetization processes, bursts of angular momentum are emitted by hot electrons[2,4] and their conversion into sub-picosecond electrical transients acts as the source of THz radiation.[17] Older pioneering works already discussed the intrinsic THz emission of pure ferromagnetic layers[18] or related to magnetic and surface nonlinearities.[19] These small signals can now be further amplified by adding an efficient spin-to-charge converter,[20] to an extent that these magnetic heterostructures can compete with optical rectification in ZnTe,[21] GaP, and InP.[22] These potentially agile and efficient THz spintronic emitters[17,20] represent the first technological implementation of femtosecond spin current bursts. Compared to polar semiconductors, such spintronic emitters require no phase matching and allow for a direct control of the polarization of the THz pulse. This new field of research is booming, and extensive work is devoted to improving and tailoring the THz emission[19] to extend the frequency range, increase efficiency, and add functionalities.

As of today, a quantitative comparison of the efficiency of the ISHE from DC to ultra-fast regimes has been addressed,[23] but despite the increasing number of published reports, IEE[24,25] remains fairly unexplored. In particular, one of the striking features of the IEE is the energy-dependent chiral band splitting,[26,27] affecting S/C interconversion rates. Therefore, when the effect is optimized for processes located at the Fermi level, nothing guarantees that it shall also work for hot electrons. This simple observation calls for a quantitative comparison of IEE effects at different timescales taking ISHE as a reference, which is the object of the present study.

The selected samples employed to answer this question are made of a $Co_{40}Fe_{40}B_{20}$ layer covered by either a 3 nm thick Pt or a 6 nm thick MgO layer, deposited on float glass and silicon substrates. The samples' magnetization was saturated with a 200 Oe applied field, as the static coercivity of the samples do not exceed 50 Oe. The reference CoFeB/Pt bilayers are known to be an efficient ISHE S/C as Pt hosts significant spin Hall effects.[14,15] The CoFeB/MgO bilayers possess Rashba split localized states within the CoFeB layer at the interface with the MgO layer, which act as an IEE S/C, as previously described.[29] CoFeB, MgO, and Pt are grown in the same sputtering chamber (Singulus) in the same batch. The exact thickness of each layer has been measured using x-ray reflectivity, and their roughness is found below 1 nm. Magnetization measurements were also carried out using vibrating-sample magnetometry and corroborated by ferromagnetic resonance (FMR). To quantify the dynamics of S/C mechanisms, our measurements focus on the injection of spin at various time scales as well as at different carriers' energies. This includes quasi-DC radio frequency (RF) spin-pumping[28] via ferromagnetic resonance (FMR) combined with ultrafast emission of hot carriers' spin currents through ultrafast demagnetization. FMR is a standard technique for probing S/C at quasi-DC frequency range when the carriers are thermalized. In our experiment, the samples are excited by a microwave magnetic field at a fixed frequency of 3.2 GHz injecting the spin current in the longitudinal direction [see Fig. 1(a)]. The FMR signal was recorded as a function of the DC magnetic field strength. In addition, we used a slow modulation of the magnetic field to enable sensitive lock-in detection, resulting in the measurements of derivatives of FMR and S/C conversion signals with respect to the magnetic field. While the net FMR signal has AC and DC components,[31] only the DC conversion signal is detected in this work.

To assess the efficiency of S/C conversion in the ultrafast regime, we perform time-dependent terahertz spectroscopy. In this experiment, we use laser pulses at 800 nm with a 150 fs duration, which are generated by an amplified Ti-sapphire laser at a 1 kHz repetition rate. The 400 nm pulses were generated by doubling the frequency of the fundamental laser wavelength. The absorption of the femtosecond laser pulse by the ferromagnetic layer and its ultrafast demagnetization (addressed in Note 6 of the supplementary material) generates a burst of spin current, which is then converted into charge through the S/C process and leads to the emission of pulsed radiation at THz frequencies.[17] The emitted terahertz (THz) radiation is measured using electro-optic sampling in a 0.5 mm thick ⟨110⟩ ZnTe crystal in air. The response function of the ZnTe detector and the duration of the probe pulse limit the THz detection to a range from 300 GHz to approximately 3 THz (see Note 1 in the supplementary material). Due to the frequency-dependent absorption of the THz radiation by the float-glass substrate, the samples were re-grown on high-resistivity silicon substrates (see Note 2 in the supplementary material). Note that all THz responses were measured at a pump fluence below 0.5 mJ/cm^2, where the amplitude of the detected THz signals is directly proportional to the incident density of optical energy. The THz signals presented in this work were recorded under equal photoexcitation of the ferromagnetic layer and were normalized by the impedance of the

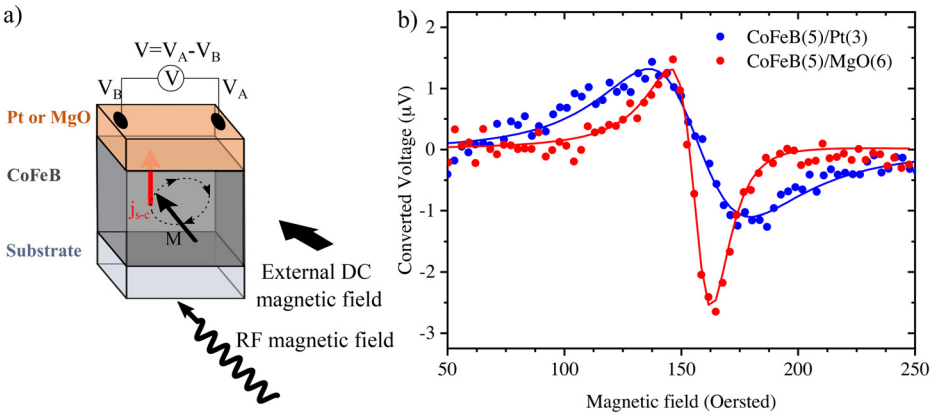

FIG. 1. (a) Schematic representation of the FMR/spin-pumping experimental configuration. (b) Raw measurements of the Spin–charge voltages at 3.8 GHz for CoFeB(5)/Pt(3) in blue and CoFeB(5)/MgO(6) in red with their respective fits. After integration and fitting, CoFeB/Pt and CoFeB/MgO conversion efficiencies are of the same order of magnitude.

respective sample (see Note 3 in the supplementary material). For the THz-emission experiments at 400 and 800 nm wavelengths, the absorbed optical fluence inside the ferromagnetic layer was kept constant (see Note 4 in the supplementary material).

First, radio frequency spin pumping experiments were carried out as shown in Fig. 1(a). The ferromagnetic resonance of the magnetic layer was recorded at 3.2 GHz as a function of the sweeping DC magnetic field. When the resonance condition of the CoFeB is met, angular momentum is absorbed, and a dynamical non-equilibrium spin population can be pumped into a nearby layer or can be accumulated at the interface with an insulator. We then measure the built-in transverse voltages across the samples resulting from the S/C conversion (as described in Ref. 29), as shown in Fig. 1(b). Built-in DC voltages across the CoFeB(5)/MgO and CoFeB(5)/Pt samples follow the FMR resonances for the same magnetic field/frequency conditions. We subsequently fit the line shapes to extract all relevant parameters: amplitude, resonance field, and linewidth. From Fig. 1(b), it is clear that CoFeB/Pt and CoFeB/MgO bilayers generate S/C voltages of the same order of magnitude. After signal integration and corrected by appropriate prefactors, such as the resonance bandwidth, one finds that Pt is only 60% more effective than MgO. This is consistent with our previous results,[29] and it underlines the presence of a Rashba electronic state at the CoFeB(5)/MgO(6) interface.[29]

We now extend the investigation to the ultrafast timescale by comparing the S/C conversion of the different systems in the THz frequency range. The symmetry of the ISHE and IEE effects in CoFeB-based bilayers is addressed by flipping the samples:[20] for a fixed direction of the external magnetic field H, we are only changing the pump pulse propagation and spin-polarized current injection direction relative to the bilayer geometry. The measurement setup is schematized in Fig. 2(a).

As a first important result, Fig. 2(b) (red and orange curves) shows that the CoFeB/MgO samples produce a THz signal that is one to two orders of magnitude lower than ISHE bilayers, in stark contrast to the RF spin pumping measurements [Fig. 1(b)]. For the Pt-based emitters [green and blue curves in Fig. 2(b)], the shape, symmetry, and spectrum of the THz signals are unchanged by the CoFeB thickness, confirming the robust ISHE nature of the S/C mechanism in Pt. In particular, this shows that possible S/C mechanisms in the bulk of FM film are much less efficient than the ISHE in Pt. In contrast, the small emitted THz signals for the MgO-based samples and their thickness dependence indicate a competition between bulk and interface effects, not observed in RF spin pumping. Aside from direct ultrafast demagnetization contributions,[18,35] ultra-fast angular momentum transport taking place *inside the ferromagnetic layers* can also induce significant contributions to the measured THz signals. Indeed, both spins and charges can diffuse (ballistically or not) under the action of temperature gradients as described through the Seebeck[36] and longitudinal spin Seebeck effects.[37–39] Even in insulators, these processes appear on the timescale of thermalization of the photoexcited electrons toward a Fermi–Dirac distribution. As a result, transverse voltages due to ultrafast anomalous Nernst effects or ISHE within the CoFeB generate THz bursts with a symmetry depending on the direction of transient temperature gradients. Therefore, these effects scale with FM thickness and are influenced by light absorption profiles, whose gradients can define the direction of the flow of photoexcited hot carriers in symmetric structures. Our measurements actually show that for the 20 nm thick CoFeB/MgO, flipping the sample does not reverse the sign of the THz emission [orange curves in Fig. 2(b)] and does not significantly affect the THz spectrum. This evidences that bulk S/C conversion processes dominate in the 20 nm thick CoFeB/MgO, as their direction is simply imposed by the instantaneous light absorption gradient (independently of the sample orientation with respect to the pump pulse propagation direction). On the other hand, the sign change for the CoFeB(5)/MgO(6) bilayer [red curves in Fig. 2(b)] clearly indicates that the S/C contribution from the bulk of the FM layer is not dominant (but may still be present) in this sample. The interfacial S/C mechanism in CoFeB(5)/MgO(6) is therefore the major effect, with

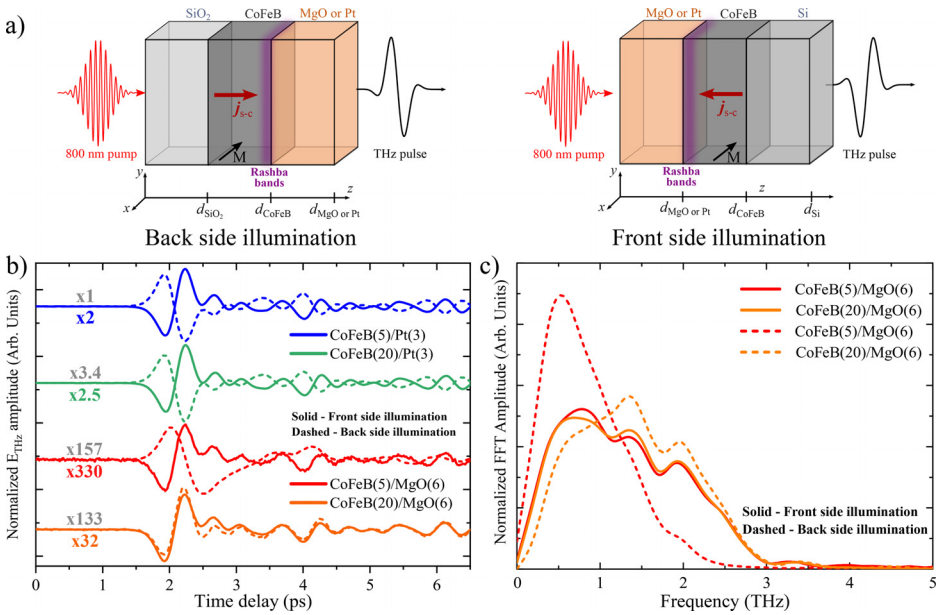

FIG. 2. Ultrafast THz emission measurements. Schematics of (a) the two THz-time domain spectroscopy experimental configurations: 800 nm pump impinging on the glass substrate side and the THz radiation collected from the bilayer side and vice versa for the samples on the silicon substrate. THz waveform recorded for the (b) four CoFeB-based systems in the two illumination configurations. Signals are shifted vertically for the sake of clarity. The multiplication factors are relative to CoFeB(5)/Pt(3) emitter amplitudes. (c) THz spectra for the MgO-based samples. Solid (dashed) lines correspond to the front (back) side illumination. The spectra are normalized by the integral over all spectral components.

the same symmetry as for the ISHE in CoFeB/Pt samples. Importantly, the reversal of the CoFeB(5)/MgO(6) pumping direction is also accompanied by a significant change in the emission spectrum [red solid and dashed lines in Fig. 2(c)], indicating that multiple competing S/C conversion mechanisms (bulk contributions vs interfacial IEE conversion) have different temporal characteristics.

We now aim to modify the injected hot carrier distribution by changing the pumping photon energy using 400 and 800 nm wavelengths. Again, we compare the interfacial IEE system of the CoFeB(5)/MgO(6) sample to the ISHE system CoFeB(5)/Pt(3). For a comparable light absorption profile and absorbed optical fluence in the 5 nm thin CoFeB layer, the change of pump wavelength should mainly affect the excited hot electron energy distributions. We observe that the ISHE emitter CoFeB(5)/Pt(3) remains insensitive to the change of pump wavelength, leading to an identical THz spectrum, shown in Fig. 3. This measurement is consistent with the literature.[30] On the other hand, both shape and spectrum of the emitted THz pulse is quite different for the CoFeB(5)/MgO(6) sample when changing the pump pulse photon energy. Interestingly, the broadening of the detected THz spectrum, when pumped with the 400 nm radiation, indicates a faster S/C conversion and suggests an energy-dependent spin-carrier relaxation rate, characteristic of the Rashba interface present in the CoFeB(5)/MgO(6) bilayer.

Our THz emission experiments also demonstrate that the CoFeB/MgO system exhibits a one to two orders of magnitude smaller ultrafast S/C signal whatever the CoFeB thickness. Moreover, only the CoFeB(5)/MgO(6) signal is consistent with the presence of an interfacial IEE S/C mechanism. Very interestingly, the spin–charge conversion characteristics of the CoFeB(5)/MgO(6) bilayer show a strong dependence on the energy of the incident pumping radiation, as well as a drastic gain of S/C efficiency in the quasi-static spin-pumping regime. Such a huge difference in S/C conversion rates for ISHE and IEE emitters between quasi-DC and sub-picosecond timescales has to stem from the S/C mechanism itself, as the spin transparency is perfect for the CoFeB/MgO systems where the Rashba state is localized inside the ferromagnet.[29] It is known that the ISHE relies on extrinsic, impurity scattering, and intrinsic mechanisms linked to the orbital momentum of the bands themselves.[9,10,32] The extrinsic contributions stem from spin–orbit coupling during scattering events leading to asymmetric skew and side-jump scattering from impurities. As electronic velocities in heavy metals (like Pt) only depend marginally on the electronic temperature above the Fermi level, the ISHE mechanism is robust for high- and low-energy spin carriers during the laser-induced magnetization changes.

In contrast, the band structure dependence of the IEE mechanism can be detrimental to the ultrafast S/C conversion, given that most well-known Rashba interfaces are mainly split only close to the Fermi level. Inside the ferromagnet, the energy distribution of the electrons carrying angular momentum is indeed highly nonlinear and band structure-dependent. It can, thus, be rather broad and even structured.[33] It was reported to spread up to about 1.5 eV from the Fermi level in the early stages of the optical excitation, with a typical center weight of around 0.2 eV for thermalized carriers at relevant timescales.[34] In addition, several bands can potentially simultaneously participate in the S/C conversion. In particular, first-principle calculations for the CoFeB/MgO interface show that the Rashba splitting is linked to specific bands relatively close to the Fermi level.[29,34] In this system, two extra Rashba splittings of opposite sign may cancel at higher energies, and only electrons close to the Fermi level can contribute to an efficient IEE S/C conversion. This energy-dependent averaging should lead to reduced THz generation efficiency, which is consistent with our measurements. In addition, the key role of the energy distribution of the angular momentum-carrying electrons in the case of IEE S/C conversion is perfectly illustrated by the pump wavelength-dependent THz emission from CoFeB(5)/MgO(6), as shown in Fig. 3. Thus, despite the observed loss of efficiency, the IEE systems may permit the tuning of THz emission bandwidth by simply changing the incident hot carrier energy, i.e., the wavelength of the exciting pump pulse.

In conclusion, we have demonstrated the drastic evolution of IEE-based spin-to-charge conversion efficiency as a function of the carriers' energy. While ISHE remains robust for both hot and thermalized spin-polarized carriers, the dramatic loss of efficiency of the inverse Edelstein systems was qualitatively explained by the energy-dependent splitting of the Rashba bands[29] and by the possible differences in spin lifetime of the hot and thermalized carriers. As a result, while THz emission can be reliably inferred from the DC behavior of ISHE materials, understanding the IEE systems requires band structure calculations complemented by the time-resolved hot carrier distribution.

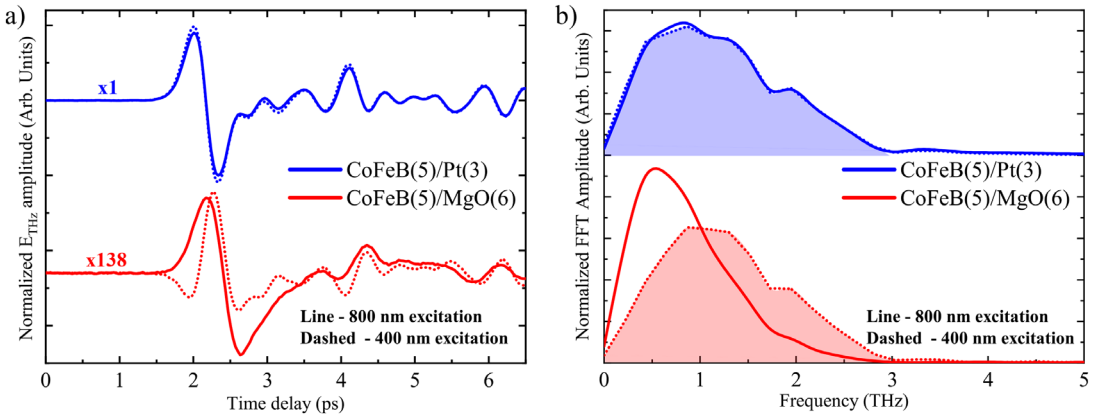

FIG. 3. Wavelength dependence of the emitted THz signals. The CoFeB(5)/MgO(6) sample, where the interfacial contribution is dominant, changes its emission spectrum with incident wavelength, underlining the sensitivity of the interfacial S/C conversion mechanism to the hot electrons' energy distribution in CoFeB(5)/MgO(6).

Nevertheless, such added complexity of the IEE devices could be used for a pump pulse wavelength-dependent modulation of the temporal profile of the spin-current bursts and subsequent control over emitted THz pulse spectrum and phase. Additionally, we propose that the efficiency of THz emission could be greatly improved using materials where the Rashba splitting is not exactly at the Fermi level, but better adapted to the energy distribution of charge and spin carriers at subpicosecond timescales.

See the supplementary material for information about the calculated response function of the THz spectrometer, THz refractive indices of the Si and SiO_2 substrates, and THz and optical properties of spintronic bilayers discussed in this work.

We acknowledge funding from the French National Research Agency (ANR) through the SANTA (No. ANR-18-CE24-0018-01), SPINUP (No. ANR-21-CE24-0026-01), and ORION (No. ANR-20-CE30-0022-03) projects, SPICY from the LabEx NanoSaclay Investissements d'Avenir Program (Reference No.: ANR-10-LABX-0035), and by Région Pays de la Loire, Grant name NanoPlasMag (No. 2017 09376).

AUTHOR DECLARATIONS

Conflict of Interest

The authors have no conflicts to disclose.

Author Contributions

Artem Levchuk: Conceptualization (equal); Formal analysis (equal); Investigation (equal); Visualization (equal); Writing – review & editing (equal). **Michel Viret:** Conceptualization (equal); Formal analysis (equal); Funding acquisition (equal); Investigation (equal); Writing – original draft (equal); Writing – review & editing (equal). **Vincent Juvé:** Conceptualization (equal); Formal analysis (equal); Funding acquisition (equal); Investigation (equal); Visualization (equal); Writing – review & editing (equal). **Tadele Orbula Otomalo:** Validation (supporting); Writing – review & editing (supporting). **Théophile Chirac:** Validation (supporting); Writing – review & editing (supporting). **Olivier Rousseau:** Validation (supporting); Writing – review & editing (supporting). **Aurélie Solignac:** Investigation (supporting); Resources (lead). **Gwenaëlle Vaudel:** Investigation (supporting); Resources (equal); Writing – review & editing (supporting). **Pascal Ruello:** Conceptualization (equal); Formal analysis (equal); Funding acquisition (equal); Investigation (equal); Writing – review & editing (equal). **Jean-Yves Chauleau:** Conceptualization (equal); Formal analysis (equal); Funding acquisition (equal); Investigation (equal); Writing – original draft (equal); Writing – review & editing (equal).

DATA AVAILABILITY

The data that support the findings of this study are available from the corresponding authors upon reasonable request.

REFERENCES

[1]S. A. Wolf, D. D. Awschalom, R. A. Buhrman, J. M. Daughton, S. von Molnár, M. L. Roukes, A. Y. Chtchelkanova, and D. M. Treger, "Spintronics: A spin-based electronics vision for the future," Science (1979) **294**, 1488 (2001).
[2]M. Battiato, K. Carva, and P. M. Oppeneer, "Superdiffusive spin transport as a mechanism of ultrafast demagnetization," Phys. Rev. Lett. **105**, 027203 (2010).
[3]A. Melnikov, I. Razdolski, T. O. Wehling, E. T. Papaioannou, V. Roddatis, P. Fumagalli, O. Aktsipetrov, A. I. Lichtenstein, and U. Bovensiepen, "Ultrafast transport of laser-excited spin-polarized carriers in Au/Fe/MgO(001)," Phys. Rev. Lett. **107**, 076601 (2011).
[4]A. Alekhin, I. Razdolski, N. Illin *et al.*, "Femtosecond spin current pulses generated by the nonthermal spin-dependent Seebeck effect and interacting with ferromagnets in spin valves," Phys. Rev. Lett. **119**, 017202 (2017).
[5]E. Beaurepaire, J.-C. Merle, A. Daunois, and J.-Y. Bigot, "Ultrafast spin dynamics in ferromagnetic nickel," Phys. Rev. Lett. **76**, 4250 (1996).
[6]J.-Y. Bigot and M. Vomir, "Ultrafast magnetization dynamics of nanostructures," Ann. Phys. **525**, 2 (2013).
[7]J. Walowski and M. Münzenberg, "Perspective: Ultrafast magnetism and THz spintronics," J. Appl. Phys. **120**, 140901 (2016).
[8]T. H. Dang, J. Hawecker, E. Rongione *et al.*, "Ultrafast spin-currents and charge conversion at 3*d*-5*d* interfaces probed by time-domain terahertz spectroscopy," Appl. Phys. Rev. **7**, 41409 (2020).
[9]J. E. Hirsch, "Spin Hall effect," Phys. Rev. Lett. **83**, 1834 (1999).
[10]J. Sinova, S. O. Valenzuela, J. Wunderlich, C. H. Back, and T. Jungwirth, "Spin Hall effects," Rev. Mod. Phys. **87**, 1213 (2015).
[11]N. Nagaosa, J. Sinova, S. Onoda, A. H. MacDonald, and N. P. Ong, "Anomalous Hall effect," Rev. Mod. Phys. **82**, 1539 (2010).
[12]J. C. R. Sánchez, L. Vila, G. Desfonds, S. Gambarelli, J. P. Attané, J. M. de Teresa, C. Magén, and A. Fert, "Spin-to-charge conversion using Rashba coupling at the interface between non-magnetic materials," Nat. Commun. **4**, 2944 (2013).
[13]S. Sangiao, J. M. de Teresa, L. Morellon, I. Lucas, M. C. Martinez-Velarte, and M. Viret, "Control of the spin to charge conversion using the inverse Rashba–Edelstein effect," Appl. Phys. Lett. **106**, 172403 (2015).
[14]E. Lesne, Y. Fu, S. Oyarzun *et al.*, "Highly efficient and tunable spin-to-charge conversion through Rashba coupling at oxide interfaces," Nat. Mater. **15**, 1261 (2016).
[15]J.-Y. Chauleau, M. Boselli, S. Gariglio, R. Weil, G. de Loubens, J.-M. Triscone, and M. Viret, "Efficient spin-to-charge conversion in the 2D electron liquid at the LAO/STO interface," Europhys. Lett. **116**, 17006 (2016).
[16]S. D. Ganichev, E. L. Ivchenko, V. V. Bel'kov, S. A. Tarasenko, M. Sollinger, D. Weiss, W. Wegscheider, and W. Prettl, "Spin-galvanic effect," Nature **417**, 153 (2002).
[17]T. Kampfrath, M. Battiato, P. Maldonado *et al.*, "Terahertz spin current pulses controlled by magnetic heterostructures," Nat. Nanotechnol. **8**, 256 (2013).
[18]E. Beaurepaire, G. M. Turner, S. M. Harrel, M. C. Beard, J. Y. Bigot, and C. A. Schmuttenmaer, "Coherent terahertz emission from ferromagnetic films excited by femtosecond laser pulses," Appl. Phys. Lett. **84**, 3465 (2004).
[19]D. J. Hilton, R. D. Averitt, C. A. Meserole, G. L. Fisher, D. J. Funk, J. D. Thompson, and A. J. Taylor, "Terahertz emission via ultrashort-pulse excitation of magnetic metal films," Opt. Lett. **29**, 1805 (2004).
[20]T. Seifert, S. Jaiswal, U. Martens *et al.*, "Efficient metallic spintronic emitters of ultrabroadband terahertz radiation," Nat. Photonics **10**, 483 (2016).
[21]A. Rice, Y. Jin, X. F. Ma, X.-C. Zhang, D. Bliss, J. Larkin, and M. Alexander, "Terahertz optical rectification from ⟨110⟩ zinc-blende crystals," Appl. Phys. Lett. **64**, 1324 (1994).
[22]M. B. Johnston, D. M. Whittaker, A. Corchia, A. G. Davies, and E. H. Linfield, "Simulation of terahertz generation at semiconductor surfaces," Phys. Rev. B: Condens. Matter Mater. Phys. **65**, 165301 (2002).
[23]M. Meinert, B. Gliniors, O. Gueckstock, T. S. Seifert, L. Liensberger, M. Weiler, S. Wimmer, H. Ebert, and T. Kampfrath, "High-throughput techniques for measuring the spin Hall effect," Phys. Rev. Appl. **14**, 064011 (2020).
[24]C. Zhou, Y. Liu, Z. Wang *et al.*, "Broadband terahertz generation via the interface inverse Rashba–Edelstein effect," Phys Rev Lett **121**, 086801 (2018).
[25]M. B. Jungfleisch, Q. Zhang, W. Zhang, J. E. Pearson, R. D. Schaller, H. Wen, and A. Hoffmann, "Control of terahertz emission by ultrafast spin-charge current conversion at Rashba interfaces," Phys. Rev. Lett. **120**, 207207 (2018).
[26]Z. Zhong, A. Tóth, and K. Held, "Theory of spin-orbit coupling at $LaAlO_3$/$SrTiO_3$ interfaces and $SrTiO_3$ surfaces," Phys. Rev. B **87**, 161102 (2013).
[27]K. V. Shanavas, "Theoretical study of the cubic Rashba effect at the $SrTiO_3$ (001) surfaces," Phys. Rev. B **93**, 045108 (2016).

[28]Y. Tserkovnyak, A. Brataas, and G. E. W. Bauer, "Spin pumping and magnetization dynamics in metallic multilayers," Phys. Rev. B **66**, 224403 (2002).
[29]O. Rousseau, C. Gorini, F. Ibrahim, J.-Y. Chauleau, A. Solignac, A. Hallal, S. Tölle, M. Chshiev, and M. Viret, "Spin-charge conversion in ferromagnetic Rashba states," Phys. Rev. B **104**, 134438 (2021).
[30]E. T. Papaioannou, G. Torosyan, S. Keller, L. Scheuer, M. Battiato, V. K. Mag-Usara, J. L'Huillier, M. Tani, and R. Beigang, "Efficient terahertz generation using Fe/Pt spintronic emitters pumped at different wavelengths," IEEE Trans. Magn. **54**, 1 (2018).
[31]C. Hahn, G. de Loubens, M. Viret, O. Klein, V. V. Naletov, and J. Ben Youssef, "Detection of the microwave spin pumping using the inverse spin Hall effect," Phys. Rev. Lett. **111**, 217204 (2013).
[32]S. Murakami, N. Nagaosa, and S. Zhang, "Dissipationless quantum spin current at room temperature," Science **301**, 1348–2016 (2003).
[33]H.-S. Rhie, H. A. Dürr, and W. Eberhardt, "Femtosecond electron and spin dynamics in Ni/W (110) films," Phys. Rev. Lett. **90**, 247201 (2003).
[34]B. Dieny and M. Chshiev, "Perpendicular magnetic anisotropy at transition metal/oxide interfaces and applications," Rev. Mod. Phys. **89**, 025008 (2017).
[35]R. Rouzegar, L. Brandt, L. Nádvorník *et al.*, "Laser-induced terahertz spin transport in magnetic nanostructures arises from the same force as ultrafast demagnetization," Phys. Rev. B **106**, 144427 (2022).
[36]K. Takahashi, T. Kanno, A. Sakai, H. Tamaki, H. Kusada, and Y. Yamada, "Terahertz radiation via ultrafast manipulation of thermoelectric conversion in thermoelectric thin films," Adv. Opt. Mater. **2**, 428 (2014).
[37]T. S. Seifert, S. Jaiswal, J. Barker *et al.*, "Femtosecond formation dynamics of the spin Seebeck effect revealed by terahertz spectroscopy," Nat. Commun. **9**(1), 2899 (2018).
[38]J. Kimling, G. M. Choi, J. T. Brangham, T. Matalla-Wagner, T. Huebner, T. Kuschel, F. Yang, and D. G. Cahill, "Picosecond spin Seebeck effect," Phys. Rev. Lett. **118**, 057201 (2017).
[39]J. E. Wegrowe, H. J. Drouhin, and D. Lacour, "Anisotropic magnetothermal transport and spin Seebeck effect," Phys. Rev. B: Condens. Matter Mater. Phys. **89**, 094409 (2014).